Physics – Uspekhi **62** (9) 920 – 930 (2019)

PHYSICS OF OUR DAYS

PACS numbers: **12.10. – g**, **12.60. – i**, **14.80. – j**

The Higgs program and open questions in particle physics and cosmology

B Heinemann, Y Nir

DOI: https://doi.org/10.3367/UFNe.2019.05.038568

Contents

Abstract. The Higgs program is relevant to many of the open fundamental questions in particle physics and cosmology. Thus, when discussing future collider experiments, one way of comparing them is by assessing their potential contributions to progress on these questions. We discuss in detail the capabilities of various proposed experiments in searching for singlet scalars, which are relevant to several of the open questions, and in measuring Higgs decays into fermion pairs, which are relevant to the flavor puzzles. With regard to other interesting questions, we list the most relevant observables within the Higgs program.

Keywords: Higgs boson, e^+e^--collider, pp-collider, flavor physics, Standard Model, baryon asymmetry of the Universe

1. Introduction

The jewel in the crown of achievements of LHC experiments to date is the discovery of the Higgs boson in July 2012 [1, 2]. The discovery of a Higgs boson is, however, not just the end of a story — a quest that began with the theoretical predictions of Brout, Englert [3], and Higgs [4] — but also the beginning of one. While the presence of the Higgs boson provides a solution to the question of how fundamental particles can acquire mass, it does not actually explain the mass values themselves, and it also raises new questions. "The Higgs program" is a major research project at the LHC and for all proposed future collider experiments. From the experimental side, the Higgs program comprises a large set of measurements aimed at learning the detailed properties of this unique particle. From the theoretical side, this is also a very exciting program, as it touches upon several open questions and puzzles in particle physics and particle cosmology.

In this article, we explore the relationship between the properties of the Higgs boson and big questions in the field of particle physics and cosmology. This work was initiated by discussions within the Scientific Policy Committee of CERN in the context of discussions on future accelerators. All proposed future accelerators consider measurements of the Higgs boson a major part of their scientific program, and this short article is designed to summarize concisely the conclusions from the currently available literature that relates Higgs precision measurements to fundamental open questions about our Universe. We also summarize the precision these future colliders are estimated to have, and try to contrast that with the precision required to answer a given question. It is worth noting that for many of the questions there are also important observables unrelated to Higgs boson measurements (in both collider and non-collider experiments), but discussing them is beyond the scope of this article.

Here is a list of seven open questions at the forefront of particle physics and cosmology, to which the Higgs program may provide answers:

(1) Is h the only scalar degree of freedom?
(2) Is h elementary?
(3) What keeps $m_h^2 \ll m_{Pl}^2$?
(4) Was the electroweak phase transition first order?
(5) Did *CP* violating h interactions generate the baryon asymmetry?
(6) Are there light SM-singlet degrees of freedom (in particular, related to Dark Matter)?

B Heinemann [1, 2, a], **Y Nir** [3, b]
[1] Deutsches Elektronen-Synchrotron, 22607 Hamburg, Germany
[2] Albert-Ludwigs-Universität Freiburg, Physikalisches Institut, 79104 Freiburg, Germany
[3] Department of Particle Physics and Astrophysics, Weizmann Institute of Science, Rehovot, 7610001 Israel
E-mail: [a] beate.heinemann@desy.de, [b] yosef.nir@weizmann.ac.il

Received 6 May 2019
Uspekhi Fizicheskikh Nauk **189** (9) 985 – 996 (2019)
DOI: https://doi.org/10.3367/UFNr.2019.05.038568

(7) What is the solution to the flavor puzzle(s)?

In what follows, we focus on two topics. In Section 3, we describe the search for singlet scalars. We choose this topic for four reasons:

• It is relevant to a large number (four) of the above questions;

• The Higgs program is likely to be the unique portal to such particles;

• The search for singlet scalars by itself constitutes a rich and broad experimental program;

• For the question of the electroweak phase transition, there is a clear target for the required accuracy that will give a definite answer to this question.

In Section 4, we discuss measurements that are relevant to the flavor puzzles. Again, there are several reasons for this choice of topic:

• The flavor puzzles are long-standing, and the Higgs program provides an opportunity to measure new flavor parameters and make progress;

• The main ingredient in the flavor-related Higgs program — the measurement of Yukawa couplings — is also relevant to other questions.

• The flavor-related measurements by themselves constitute a rich and broad experimental program;

• In contrast to the question of the electroweak phase transition, for the flavor measurements there is no lower bound on the size of new physics effects. Instead, the better the accuracy, the higher the scale of new physics to which there is sensitivity.

All other topics are discussed briefly in Section 5, where we describe the most relevant experimental measurements to each physics question but do not compare the capabilities of the various experiments (which is still a work in progress). In Section 6, we present three important conclusions about the scientific significance of the Higgs program.

2. Experiments

For the purpose of discussing the expected accuracy of future measurements, the following future collider parameters (integrated luminosity $\mathcal{L}$, center of mass energy $\sqrt{s}$, and, where relevant, polarization) are assumed:

• HL-LHC: pp collider, $\mathcal{L} = 3 - 4$ ab^{-1} at $\sqrt{s} = 14$ TeV (2026 to late 2030s: $\gtrsim 10$ years) [5].

• ILC: e^+e^- collider, with e^- 80% polarized and e^+ 30% polarized, to be operated in two stages (22 years total, including shutdowns) [6]:

1. ILC250: $\mathcal{L} = 2$ ab^{-1} at $\sqrt{s} = 250$ GeV (11 years),
2. ILC500: $\mathcal{L} = 4$ ab^{-1} at $\sqrt{s} = 500$ GeV (10 years). This also includes a 1-year run at $\sqrt{s} = 365$ GeV.

• CLIC: e^+e^- collider, with e^- 80% polarized and e^+ not polarized, to be operated in three stages (26 years, including shutdowns) [5]:

1. CLIC380: $\mathcal{L} = 1.0$ ab^{-1} at $\sqrt{s} = 380$ GeV (8 years),
2. CLIC1500: $\mathcal{L} = 2.5$ ab^{-1} at $\sqrt{s} = 1400$ GeV (7 years),
3. CLIC3000: $\mathcal{L} = 5.0$ ab^{-1} at $\sqrt{s} = 3000$ GeV (7 years).

• CEPC: e^+e^- collider, without polarization, $\mathcal{L} = 5.6$ ab^{-1} at $\sqrt{s} = 240$ GeV (7 years) [7]. It is assumed that there are two experiments collecting the data, and the datasets are combined.

• FCC-ee: e^+e^- collider, without polarization, to be operated in two stages [5]:

1. FCC240: $\mathcal{L} = 5.0$ ab^{-1} at $\sqrt{s} = 240$ GeV (3 years),
2. FCC365: $\mathcal{L} = 1.5$ ab^{-1} at $\sqrt{s} \approx 365$ GeV (5 years).

In both cases it is assumed that there are two experiments collecting the data, and the datasets are combined.

• LHeC: ep collider, colliding 7-TeV HL-LHC protons with 60-GeV electrons, aiming to deliver $\mathcal{L} = 1$ ab^{-1} within 12 years. For the last 4 years, the HL-LHC is assumed not to operate concurrently for pp collisions [5].

• HE-LHC: pp collider, $\mathcal{L} = 10$ ab^{-1} at $\sqrt{s} = 27$ TeV (20 years) [5]. For the numbers presented in Table 7, $\mathcal{L} = 15$ ab^{-1} is considered, corresponding to two collider experiments combining at least 75% of the data [8].

• FCC-hh: pp collider, $\mathcal{L} = 20$ ab^{-1} at $\sqrt{s} = 100$ TeV (25 years) [5]. For the numbers presented in Table 7, $\mathcal{L} = 30$ ab^{-1} is considered, corresponding to two collider experiments combining at least 75% of the data [8].

• Muon collider: a muon collider is also a very interesting option to collide leptons at very high energies. This is, however, not considered in this report, as the studies related to this are currently less advanced.

3. Singlet scalars

One of the experimentally most challenging extensions of the Standard Model (SM), yet one that is relevant to many interesting Higgs-related questions, is that of a singlet scalar. In fact, it appears with relation to four of the seven open questions that we posed:

(1) Is h alone?
(2) What keeps $m_h^2 \ll m_{Pl}^2$?
(3) Was the electroweak phase transition first order?
(4) Are there light SM-singlet degrees of freedom?

The simplest extension is to add to the SM a real scalar field $S(x)$ in the $(1,1)_0$ (gauge-singlet) representation. The most general renormalizable Lagrangian is [9–11] (we use the notations of [9])

$$\mathcal{L} = \mathcal{L}_{SM} + \frac{1}{2}(\partial_\mu S)(\partial^\mu S) - \frac{m_s^2}{2}S^2 - \frac{a_s}{3}S^3 - \frac{\lambda_s}{4}S^4 - \lambda_{hs}\Phi^\dagger\Phi S^2 - 2a_{hs}\Phi^\dagger\Phi S\,, \quad (1)$$

where Φ is the Higgs doublet in the $(1,2)_{+1/2}$ representation. In the general case, both Φ and S can acquire VEVs:

$$\langle\Phi\rangle = \left(0, \frac{v}{\sqrt{2}}\right), \quad \langle S\rangle = v_s\,, \quad (2)$$

and the Higgs and singlet fields mix:

$$\sin 2\theta = \frac{4v(a_{hs} + \lambda_{hs}v_s)}{M_h^2 - M_s^2}\,, \quad (3)$$

where M_h and M_s are the mass eigenvalues of the two scalar mass eigenstates ($M_h \simeq 125$ GeV).

Deviations from the SM predictions for various couplings are often parameterized by "κ parameters":

$$\kappa_x \equiv \frac{g_{hxx}}{g_{hxx}^{SM}}\,. \quad (4)$$

Within the SM extended by singlet scalars, the couplings of the Higgs boson to all fermion and vector boson pairs are modified by a universal factor. (For a discussion, see Section I of Ref. [10].) Defining δg_h via

$$\kappa_x \equiv 1 + \delta g_h\,, \quad (5)$$

we have [9]

$$\delta g_{\rm h} \approx (\cos\theta - 1) - \frac{|a_{\rm hs} + \lambda_{\rm hs} v_{\rm s}|^2}{8\pi^2}\, I_B(M_{\rm h}^2; M_{\rm h}^2, M_{\rm s}^2) - \frac{|\lambda_{\rm hs}|^2 v^2}{16\pi^2}\, I_B(M_{\rm h}^2; M_{\rm s}^2, M_{\rm s}^2)\,, \quad (6)$$

where [12]

$$I_B(p^2; m_1^2, m_2^2) = \int_0^1 {\rm d}x\, \frac{x(1-x)}{x(1-x)\,p^2 - x m_1^2 - (1-x)\,m_2^2}\,. \quad (7)$$

As concerns Eqn (6), we emphasize the following points:

• The first term on the right-hand side (RHS) is a consequence of the mixing (see Eqn 3).

• The second and third terms are a consequence of the wave function renormalization of the Higgs at one loop.

Usually, the first term dominates. This is not the case, however, in models where a Z_2 symmetry, under which $S(\Phi)$ is odd (even), is imposed. This scenario is considered the most difficult one for finding experimental evidence for a first order electroweak phase transition [11]. In this model, we have $a_{\rm hs} = v_{\rm s} = 0$ and consequently $\theta = 0$, so that the first two terms in Eqn (6) vanish. It follows that [12]

$$\delta g_{\rm h}^{(Z_2)} = -\frac{|\lambda_{\rm hs}|^2 v^2}{16\pi^2}\, I_B(M_{\rm h}^2; M_{\rm s}^2, M_{\rm s}^2) = -\frac{|\lambda_{\rm hs}|^2 v^2}{16\pi^2 M_{\rm h}^2}\left[1 - \frac{4M_{\rm s}^2 \arctan\left(\sqrt{M_{\rm h}^2/(4M_{\rm s}^2 - M_{\rm h}^2)}\right)}{\sqrt{M_{\rm h}^2(4M_{\rm s}^2 - M_{\rm h}^2)}}\right]. \quad (8)$$

In the limit $M_{\rm s}^2 \gg M_{\rm h}^2$ [12],

$$\delta g_{\rm h}^{(Z_2)} \to +\frac{|\lambda_{\rm hs}|^2 v^2}{96\pi^2 M_{\rm s}^2}\,. \quad (9)$$

3.1 $M_{\rm s} < M_{\rm h}/2$

If $M_{\rm s} < M_{\rm h}/2$, then a new decay channel for the Higgs boson opens up, h → SS, with

$$\Gamma({\rm h} \to {\rm SS}) = \frac{\lambda_{{\rm h}SS}^2}{8\pi M_{\rm h}} \sqrt{1 - \frac{4M_{\rm s}^2}{M_{\rm h}^2}}, \quad (10)$$

and

$$\lambda_{{\rm h}SS} = +c_\theta^3 \lambda_{\rm hs} v + c_\theta^2 s_\theta (a_{\rm s} + 3\lambda_{\rm s} v_{\rm s} + 2\lambda_{\rm hs} v_{\rm s} - 2a_{\rm hs}) + c_\theta s_\theta^2 (3\lambda_{\rm h} v - 2\lambda_{\rm hs} v) + s_\theta^3 (\lambda_{\rm hs} v_{\rm s} + a_{\rm hs})\,. \quad (11)$$

In the Z_2 limit,

$$\lambda_{{\rm h}SS} = \lambda_{\rm hs} v\,, \quad (12)$$

and, furthermore, S is stable, and, therefore, the h → SS mode contributes to h → invisible. Reference [13] collected the upper bounds and projections on BR(h → invisible). We quote updated results and future projections in Table 1.

The BR(h → invisible) is determined directly by analyses searching for a Higgs boson produced in association with a Z boson (at lepton and hadron colliders) or with forward jets (in the VBF process at hadron colliders) and the Higgs boson decaying invisibly, which is observed as missing transverse momentum in experiments. Several e^+e^- colliders are able to probe this with a precision of 0.3%. The best sensitivity is achieved by FCC_{hh} at 0.025%.

Table 1. Current upper bounds and projections on $BR_{inv} \equiv BR(h \to \text{invisible})$ and $BR_{und} \equiv BR(h \to \text{undetected})$.

Collider	$\sqrt{s}$, TeV	$\mathcal{L}$, ab^{-1}	BR_{inv}, %	BR_{und}, %
LHC1	7, 8	0.022	37	20
LHC2	13	0.036	26	—
LHC3	13	0.300	8.8 (68%)	7.6 (68%)
HL-LHC	14	3	2.6	2.5
CLIC	0.38	1	0.69 (90%)	1.6
CEPC	0.25	5.6	0.3	1.0
ILC	0.5	2	0.3	1.5
FCC_{ee}	0.24	5	0.3	0.87
FCC_{hh}	100	20	0.025	—

All upper bounds are given at 95% CL unless explicitly stated. The LHC2 line updates the most recent bounds from CMS [14] and ATLAS [15]. Projections for future colliders are also shown: CLIC [16], CEPC [7], ILC [17], and FCC_{ee} and FCC_{hh} [8]. For FCC_{hh}, the SM background from $H \to 4\nu$, corresponding to a BR of 0.113%, has been subtracted and the limit refers to additional invisible new physics contributions. For the LHC and HL-LHC, BR_{und} is inferred, assuming $\kappa_Z \leqslant 1$. The symbol '–' means that no value is available in the literature.

When no Z_2 symmetry is imposed and, in particular, $\sin\theta \neq 0$, the mass eigenstate S inherits the Higgs couplings, suppressed by $\sin\theta$:

$$\lambda_{Sf\bar{f}} = \sin\theta\; y_f^{\rm SM}\,, \quad (13)$$

where $y_f^{\rm SM}$ is the corresponding SM Yukawa coupling. The h → SS decay will be followed by $S \to f\bar{f}$, where $m_f < M_{\rm s}/2$ with the coupling given by Eqn (13). There are two complementary ways of searching for these decays. The first is a direct search for the final four fermion state, which we discuss further below. The second is an indirect search, via a global fit to the Higgs couplings, which can reveal (or constrain) a contribution to the Higgs width that is not accounted for by the final states that are included in the fit [13, 18, 19], the so-called

$$\text{h} \to \text{undetected}\,. \quad (14)$$

Upper bounds on BR(h → undetected) are given in Table 1, and put an upper bound on $\sin^2\theta$ for a given $M_{\rm s}$. The branching ratios to 'undetected' final state are derived from the observed cross sections and branching ratios using certain constraints. For the LHC and HL-LHC, this can only be done if $\kappa_Z \leqslant 1.0$ is assumed, which holds for singlets with $M_{\rm s} < M_{\rm h}/2$ if the dominant effect is due to $\sin\theta \neq 0$ (and in general only holds for a fraction of new physics models). For e^+e^- colliders, it is possible to use a much more direct and very model-independent constraint [13], $BR(h \to \text{undetected}) \leqslant 1 - (1 - 2\delta_\kappa)^2$, where δ_κ is the precision of the measurement of κ_Z (CLIC380: 0.4%, CEPC: 0.25%, ILC: 0.38%, FCCee: 0.22%).

Examples of other relevant experimental searches are collected in Table 2. For the μμbb final state, it is expected that the HL-LHC [20] will have a sensitivity down to $BR(h \to \mu^+\mu^- b\bar{b}) \sim 5 \times 10^{-5}$. For other decays, no projections are available.

The total width of h is, on the one hand, suppressed by the suppression of the h-couplings to pairs of SM particles but, on the other hand, enhanced by the addition of the h → SS

Table 2. Upper bounds on $(\sigma_h/\sigma_h^{SM})\,BR(h \to SS \to \overline{f_1}f_1\overline{f_2}f_2)$

$\overline{f_1}f_1\overline{f_2}f_2$	M_s, GeV	Upper bound	References
ττbb	15–60	0.03–0.12	CMS [21]
μμbb	25–63	$(1–8)\times10^{-4}$	CMS [22], ATLAS [23]
ττττ	9–15	0.2–0.3	CMS [22]
μμττ	25–63	$(1–5)\times10^{-4}$	CMS [22, 24]
γγjj	20–60	0.034–0.173	ATLAS [25]

channel. It thus provides an interesting observable to probe this scenario.

The width of the h boson can be inferred in the LHC using three methods:

• The cross section of off-shell h-boson production is proportional to $[(s - M_h^2)^2 + M_h^2\Gamma_h^2]^{-1}$. Measuring it at different values of s allows an extraction of the width under the assumption that the couplings of h to the particles involved are independent of s (this is not a good assumption for several BSM models). The most precise extraction [26] has been done in the ZZ decay mode by the CMS collaboration using ~ 80 fb^{-1} of run-2 data, and gives $3.2^{+2.8}_{-2.2}$ MeV. It is foreseen that, with the HL-LHC and improvements in the theoretical calculations, Γ_h will be extracted with a precision of 20% using this method [27].

• Using the diphoton decay mode, it is also possible to determine the width through interference effects. This is complementary, as well as theoretically robust, and will be able to probe values of $(8 - 22) \times \Gamma_h$ [27].

• Using the coupling measurements and assuming that $\kappa_Z \leqslant 1$ (which holds if the dominant effect is due to $\sin\theta \neq 0$), Γ_h can be extracted with a precision of 5% with the HL-LHC. This determination of the width is only possible if one assumes that there are no undetected final states. We can either fix the width and determine the BR to undetected particles or we can set the latter to zero and determine the width.

In e^+e^- colliders, Γ_h can be measured based on $\sigma(e^+e^- \to Zh)$ and $BR(h \to ZZ^*)$:

$$\frac{\sigma(e^+e^- \to Zh)}{BR(h \to ZZ^*)} = \frac{\sigma(e^+e^- \to Zh)}{\Gamma(h \to ZZ^*)/\Gamma_h} = \left[\frac{\sigma(e^+e^- \to Zh)}{\Gamma(h \to ZZ^*)}\right]_{SM}\Gamma_h\,, \tag{15}$$

where we used the fact that, within the framework discussed here, both $\sigma(e^+e^- \to Zh)$ and $\Gamma(h \to ZZ^*)$ are modified from their SM values by the same factor, κ_Z^2. The precision of this determination is then limited by the statistics of $h \to ZZ^*$ decays. Both the statistical precision and the model dependence can be reduced significantly if also $\sigma(e^+e^- \to h\nu_e\nu_e)$ and $BR(h \to WW^*)$, as is possible for FCC_{ee} at 365 GeV, CLIC (at all proposed energies), and ILC at 500 GeV. This explains the substantial improvement observed when higher energy data are included.

The estimated sensitivities of future e^+e^- colliders to the total width are given in Table 3. They are far superior to the first and second determinations of the width at the LHC discussed above. A word of caution is, however, in place here. While the assumption that both the Zh cross section and the $h \to ZZ$ decay width are modified by one simple factor, κ_Z^2, holds in the framework discussed in this subsection (extending the SM with a single light real singlet scalar), it is a model-dependent assumption and cannot be assumed in general [17]. Thus, for ILC, the width has been extracted using an EFT fit with the use of polarization and angular information instead. This is the reason that we also quote the method used in each experiment in Table 3.

Table 3. Precision of Γ_h for the following e^+e^- colliders: CLIC [16], CEPC [7], ILC [6], and FCC_{ee} [8].

Collider	$\sqrt{s}$, TeV	$\mathcal{L}$, ab^{-1}	$\delta\Gamma_h/\Gamma_h$, %	method
CLIC 380	0.38	1.0	4.7	κ
CLIC 1.5	0.38 + 1.5	2.5	2.6	κ
CLIC 3.0	0.38 + 1.5 + 3	5	2.5	κ
ILC 250	0.25	2.0	2.4	Effective field theory
ILC 500	0.25 + 0.5	2.0 + 4.0	1.6	Effective field theory
CEPC	0.25	5.6	2.8	κ
FCC_{ee} 240	0.24	5.0	2.7	κ
FCC_{ee}	0.24 + 0.365	6.5	1.3	κ

3.2 $M_s > M_h/2$

The case of $M_s > M_h/2$ is more challenging. Here, there is a universal modification of all hxx couplings (see Eqn (6)). The partial width into any SM final state, $\Gamma(h \to f)$, as well as the total Higgs width, Γ_h, change by the same factor, $(1 + \delta g_h)^2$. Consequently, the branching ratios into the various final states are unchanged from the SM, but the production rates are modified:

$$\mu_i^f \equiv \frac{\sigma_i(pp \to h) \times BR(h \to f)}{[\sigma_i(pp \to h) \times BR(h \to f)]_{SM}} = (1 + \delta g_h)^2\,. \tag{16}$$

Here, i is the Higgs production mode (ggF, VBF, etc.). If there is no Z_2 symmetry, then doublet-singlet mixing is allowed, i.e., $\sin 2\theta \neq 0$ [see Eqn (3)], and the dominant contribution to δg_h in Eqn (6) is likely to come from the $(\cos\theta - 1)$ term, and consequently

$$\mu_i^f \approx \cos^2\theta\,. \tag{17}$$

If there is an unbroken Z_2 symmetry,

$$(\mu_i^f)^{(Z_2)} = 1 - \frac{|\lambda_{hs}|^2 v^2}{8\pi^2}\, I_B(M_h^2; M_s^2, M_s^2)\,. \tag{18}$$

For $M_s^2 \gg M_h^2$, we have

$$(\mu_i^f)^{(Z_2)}(M_s^2 \gg M_h^2) \approx 1 + \frac{|\lambda_{hs}|^2}{48\pi^2}\,\frac{v^2}{M_s^2}\,. \tag{19}$$

Under the assumption that the values of the signal strengths μ_i^f are the same for all production processes i and decay channels f, a fit to the ATLAS and CMS data at $\sqrt{s} = 7$ and 8 TeV, with μ as the parameter of interest, results in the best fit value [28]:

$$\mu = 1.09^{+0.11}_{-0.10}\,. \tag{20}$$

With the full HL-LHC dataset, LHC now projects, for the two best measured production rates, 1.6% for the ggF channel and 3.1% for the VBF channel. There is still a question of theory uncertainties on the ggF and VBF cross sections. One can argue that the theory precision on VBF will be $\lesssim 1\%$, while for ggF this is harder to estimate. In principle,

Table 4. Precision of the dominant Higgs production cross sections for the following e^+e^--colliders: CLIC [16], CEPC [7], ILC [17], and FCC_{ee}.

Collider	$\sqrt{s}$, TeV	$\mathcal{L}$, ab^{-1}	$\delta\sigma_{Zh}/\sigma_{Zh}$, %
CLIC	0.38	1.0	1.3
ILC	0.25	2.0	0.7
CEPC	0.25	5.6	0.5
FCC_{ee}	0.24	5.0	0.5

the above numbers already fold in acceptance uncertainties due to theory but not yet overall normalization uncertainties.

As concerns ILC, Ref. [17] (Table 6) estimates the accuracy for σ_{Zh} to be 0.7%, while for CEPC and FCC_{ee} a precision of 0.5% is expected. The accuracy of the measurement of σ_{Zh} in various proposed e^+e^- colliders is presented in Table 4.

A particularly interesting issue in which the addition of a singlet scalar to the SM is relevant is the possibility that its coupling to the Higgs field makes the EWPT first order. Ref. [29] obtains the lower bound on $|\lambda_{hs}|^2/M_s^2$ to be such that

$$\mu_i^f - 1 \gtrsim 0.6\% \,. \tag{21}$$

We conclude that ILC, CEPC, and FCC_{ee} may be able to lend support to or rule out this scenario as they reach a precision of 0.5–0.7%. However, the sensitivity may only be at the level of one standard deviation for all three colliders if the deviation is near its lower bound.

At CLIC, this scenario has been studied in detail [73] and it was estimated that, based on the Higgs coupling measurements, a constraint of

$$\mu_i^f - 1 \lesssim 0.24\% \quad \text{at} \quad 95\% \quad \text{confidence level} \tag{22}$$

can be derived when including all stages, making it sensitive to probing the order of the EWPT.

The width measurements presented in Table 3 are also sensitive to this scenario, but the precision is inferior to that of the total cross sections.

4. What is the solution to the flavor puzzle(s)?

There are several reasons to study flavor physics via Higgs physics. First, flavor physics raises three puzzles [30]:

• The Standard Model flavor puzzle: Why is there structure (smallness and hierarchy) in the charged fermion masses and the CKM mixing angles?

• The neutrino flavor puzzle: Why, in contrast to the charged fermions, does there seem to be no structure (no hierarchy, degeneracy, or smallness) in the neutrino-related flavor parameters?

• The new physics flavor puzzle: If there is new physics at the TeV scale, what is the mechanism (alignment and/or degeneracy) that prevents it from significantly modifying the SM predictions for flavor-changing neutral current (FCNC) processes?

Various models have been suggested to answer one or more of these questions. The best hope to make further progress is by measuring new flavor parameters (beyond the matrix elements of the CKM matrix). Measurements of the Yukawa couplings of h provide such an opportunity.

Second, within the Standard Model (SM), flavor changing neutral current processes are suppressed by three factors:

• Loop suppression;

• CKM suppression;

• GIM suppression.

This unique situation allows the measurements of FCNC processes to probe new physics at very high scales. The search for Higgs-related flavor violating processes, such as $t \to ch$ or $h \to \tau\mu$, provides a new arena for FCNC measurements.

Within the SM, there is a clear prediction for the tree-level values of the Yukawa couplings:

$$Y_F = \left(\frac{\sqrt{2}}{v}\right) M_F \qquad (F = U, D, E) \,. \tag{23}$$

This relation between the Yukawa matrices and the mass matrices encompasses, in fact, three features:

• Proportionality: The diagonal Yukawa couplings ($y_f \equiv Y_{ff}$) are proportional to the corresponding masses. For example,

$$\frac{y_\mu}{y_\tau} = \frac{m_\mu}{m_\tau} \,. \tag{24}$$

• Factor of proportionality: The factor that connects the mass to the diagonal Yukawa coupling is $\sqrt{2}/v$. For example,

$$y_\tau = \left(\frac{\sqrt{2}}{v}\right) m_\tau \,. \tag{25}$$

• Diagonality: The off-diagonal Yukawa couplings vanish. For example,

$$Y_{\mu\tau} = 0 \,. \tag{26}$$

The three examples in Eqns (24), (25), and (26) demonstrate that, by measuring (or constraining) the rates of $h \to \tau\tau$, $h \to \mu\mu$, and $h \to \tau\mu$, we can test each of the three features predicted by the SM separately. If deviations from the SM predictions are established, the pattern of deviations will allow us to distinguish between various frameworks that aim to solve the flavor puzzles. This is demonstrated in Table 5, where the predictions of various flavor models for the Yukawa couplings are given (adapted from [31]). In this table, the scale Λ is the one that suppresses dimension-six terms in the SM effective-field-theory (SM-EFT) of the form

$$\frac{z_{ij}}{\Lambda^2} (\Phi^\dagger \Phi) \overline{L_i} \tilde{\Phi} E_j \,, \tag{27}$$

where L_i are the lepton doublet fields in the $(1,2)_{-1/2}$ representation, and E_j are the lepton singlet fields in the $(1,1)_{-1}$ representation.

In Table 6, we present the predictions in various theoretical models for flavor-changing $t \to hq$ decays. The

Table 5. Predictions for di-lepton Higgs decays in various flavor models: SM, natural flavor conservation (NFC), minimal supersymmetric SM (MSSM), minimal flavor violation (MFV), Froggatt–Nielsen (FN) models, and Giudice–Lebedev (GL). (See [31] for details.)

Model	$\frac{y_\tau}{\sqrt{2}m_\tau/v}$	$\frac{y_\mu/y_\tau}{m_\mu/m_\tau}$	$\frac{\mathrm{BR}(h \to \mu\tau)}{\mathrm{BR}(h \to \tau\tau)}$
SM	1	1	0
NFC	$V_{hl}^* v/v_l$	1	0
MSSM	$\sin\alpha/\cos\beta$	1	0
MFV	$1 + \mathcal{O}(v^2/\Lambda^2)$	$1 + \mathcal{O}(m_\tau^2/\Lambda^2)$	0
FN	$1 + \mathcal{O}(v^2/\Lambda^2)$	$1 + \mathcal{O}(v^2/\Lambda^2)$	$\mathcal{O}(\lvert U_{23}\rvert^2 v^4/\Lambda^4)$
GL	3	5/3	$\mathcal{O}[(25/9)(m_\mu^2/m_\tau^2)]$

Table 6. Predictions BR(t → hq) (q = u, c) in various models. (See [32–34] for details.)

	SM	2HDM	MSSM	RS	SM-EFT(MFV)	SM-EFT(FN)
t → hc	3×10^{-15}	2×10^{-3}	$\leqslant 10^{-5}$	$\leqslant 10^{-4}$	$y_b^4 (V_{cb} V_{tb})^2 (v/\Lambda)^4$	$\lvert V_{cb}\rvert^2 (v/\Lambda)^4$
t → hu	2×10^{-17}	6×10^{-6}	$\leqslant 10^{-5}$	—	$y_b^4 (V_{ub} V_{tb})^2 (v/\Lambda)^4$	$\lvert V_{ub}\rvert^2 (v/\Lambda)^4$

Table 7. Experimental status and future projections of diagonal Yukawa couplings y_f and the accuracy estimated for future experiments in %.

Observable	Current range	HL-LHC	ILC250	ILC250 + 500	CLIC380	CLIC3000	CEPC	FCC240	FCC365	LHeC
		$\delta y/y$ (%)								
y_t/y_t^{SM}	$1.02^{+0.19}_{-0.15}$ [35] $1.05^{+0.14}_{-0.13}$ [36]	3.4	—	6.3	—	2.9	—	—	—	—
y_b/y_b^{SM}	$0.91^{+0.17}_{-0.16}$ [35] $0.85^{+0.13}_{-0.14}$ [36]	3.7	1.0	0.60	1.3	0.2	1.0	1.4	0.67	1.1
y_τ/y_τ^{SM}	0.93 ± 0.13 [35] 0.95 ± 0.13 [36]	1.9	1.2	0.77	2.7	0.9	1.2	1.4	0.78	1.3
y_c/y_c^{SM}	< 6.2 [40, 41]	< 220	1.8	1.2	4.1	1.3	1.9	1.8	1.2	3.6
y_μ/y_μ^{SM}	$0.72^{+0.50}_{-0.72}$ [35] < 1.63 [36]	4.3	4.0	3.8	—	5.6	5.0	9.6	3.4	—
y_e/y_e^{SM}	< 611 [42]	—	—		—	—	—	—	$< 1.6^{(+)}$	—

The accuracy quoted for future experiments is based on combining those data with the HL-LHC, except for CLIC and FCC240, where only the accuracy of the future collider is stated. Upper bounds are given at a 95% confidence level. The first line in each row shows the CMS result and the second line the ATLAS result. In both cases, a BSM contribution is allowed, the γγ and gg loop processes are treated with effective couplings, and the $Z\gamma$ process is resolved. For e^+e^- colliders, the same assumptions about the loops are made when using the so-called κ-framework. For LHC and HL-LHC [27], $BR_{BSM} = 0$ is assumed. For ILC, an EFT fit is used to extract the values and the values are combined with HL-LHC [6]. For all other colliders, the κ-fit results are quoted from Refs [7, 8, 37, 39], and no combination with HL-LHC is made. For the FCC-ee, an upper limit of 1.6 can be set on y_e/y_e^{SM} if one year of running at $\sqrt{s} \approx m_h$ is performed. When no value is available in the literature, a — is shown.

numerical estimates for the SM, 2HDM, MSSM, and RS frameworks are taken from Ref. [32] (Table 1–7). The parametric suppression factors in the SM-EFT subject to minimal flavor violation (MFV) or to Froggatt–Nielsen (FN) selection rules are taken from Refs [33] and [34], respectively.

In the following, the current measurements and expected accuracy of future measurements for the parameters relevant to flavor are discussed. For this purpose, we assume the future collider parameters presented in Section 2.

The present status of the measured y_f values is presented in Table 7, and its compatibility with the SM prediction of proportionality is presented in Fig. 1. Different methods are used for the various colliders to extract the couplings, leading to some model-dependence at the level of $(0.5 - 1.0)\%$. For third generation fermions, the current LHC precision is about $(10 - 25)\%$. With HL-LHC, it will be improved to $(2 - 4)\%$. Other future machines will improve the precision by another factor of ~ 3.

For second (and first) generation fermions, currently only upper limits are available. As concerns y_μ, the HL-LHC will measure it to better than 5%, and future e^+e^- colliders are not expected to improve this further significantly. FCC_{hh} will be able to measure the ratio $BR(h \to \mu\mu)/BR(h \to 4\mu)$ with a precision of 1.3%. Regarding y_c, the HL-LHC expected to be sensitive to values 6–21 times larger than the SM value. Future colliders will probe it in earnest with a precision of (1–2)%. At hadron colliders, it is expected that very large anomalous values of the strange quark coupling can be probed on $\phi\gamma$ decays [27]: for HL-LHC (FCC) the sensitivity is $-35 < y_s/y_b^{SM} < 57$ $(-2 < y_s/y_b^{SM} < 24)$. At e^+e^- colliders, values of $\mathcal{O}(10)\times$SM rates might be in reach [38]. With respect to the first generation, the best hope for probing the SM value of y_e directly is to run one of the circular e^+e^- colliders at $\sqrt{s} \approx m_h$ for several years. For up and down quarks, the projected sensitivity of the HL-LHC is more than 1000 times the SM value, and is only obtained indirectly.

The GL model (see Table 5) is already ruled out by the current data presented in Table 7 (by both the y_τ measurement and the y_μ upper limit). For the FN model, the current constraints imply a lower bound on the scale of new physics, $\Lambda/\sqrt{z_{\tau\tau}} \gtrsim 600$ GeV. The expected precision of HL-LHC will increase the reach to $\Lambda/\sqrt{z_{\tau\tau}} \sim 2$ TeV, while some of the future facilities can reach up to about $\Lambda/\sqrt{z_{\tau\tau}} \sim 4$ TeV.

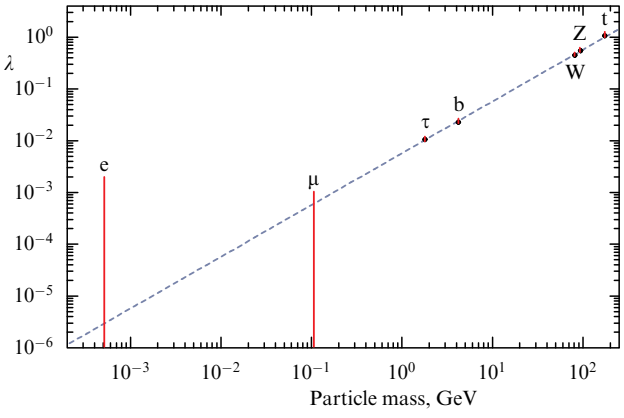

Figure 1. Currently allowed experimental ranges for Higgs couplings. For the Yukawa couplings, we present $\kappa_f m_f/v$. For the coupling to the electroweak vector bosons, we present $\sqrt{\kappa_V} m_V/v$. The SM prediction is presented by the diagonal solid line. (Keith Ellis, private communication.)

Table 8. Experimental status of measurements that depend on off-diagonal Yukawa couplings (assuming SM production rates). The LHC $t \to qh$ measurements are based on 36.1 fb^{-1}. For FCC_{hh}, the range quoted for $t \to qh$ reflects the size of the systematic uncertainty on the background of (0–5)%.

Observable	Upper bound	HL-LHC	FCC-hh
$BR(t \to ch)$	1.1×10^{-3} [43]	10^{-4} [44]	$(4.9–16)\times10^{-6}$ [8]
$BR(t \to uh)$	1.2×10^{-3} [43]	10^{-4} [44]	$(2.5–28)\times10^{-6}$ [8]
$BR(h \to \tau\mu)$	2.5×10^{-3} [45, 46]	5×10^{-4} [27]	—
$BR(h \to \tau e)$	6.1×10^{-3} [45, 46]	5×10^{-4} [20]	—
$BR(h \to \mu e)$	3.4×10^{-4} [47]	—	—

The present status of measurements and future projections for off-diagonal branching ratios are given in Table 8. At present, most upper limits are between 0.1% and 1%. With HL-LHC, they will be improved by an order of magnitude to about 1×10^{-4}. For $t \to qh$ decays, it can be expected that the sensitivity of future e^+e^- colliders to branching ratios is of the order of 10^{-5}, similar to other rare decay modes of the top quark [8], but no dedicated study is available. With FCC-hh, an improvement by another 1–2 orders of magnitude is expected, depending on the systematic uncertainties that will be obtained. These values are somewhat interesting in view of theories beyond the SM (see Table 6).

Finally, let us mention that, while the third generation couplings are already constrained to be within about 10% of the SM values, large deviations might still arise in measurements of the Yukawa couplings of the first two generations and of flavor changing decays. The experimental effort to search for these decays thus has the potential to make surprising discoveries, even if the sensitivity is far from the SM predictions.

5. Additional Questions

5.1 Is h alone?

Within the SM, there is a single real scalar field, the Higgs boson h_{SM}. It originates from a field $\Phi(1,2)_{1/2}$ that is a doublet of the SU(2) gauge symmetry. In the unitary gauge, the Higgs field is given by

$$\Phi = \begin{pmatrix} 0 \\ \dfrac{1}{\sqrt{2}}\,(v + h_{SM}) \end{pmatrix}. \tag{28}$$

The scalar h discovered in the ATLAS and CMS experiments [1, 2] has measured properties that are all consistent, within present experimental accuracy, with the SM predictions for the Higgs boson [28]. The question that is being asked is whether the observed Higgs boson is the SM Higgs boson. In fact, one can separate this question into two:

(1) Does h originate purely from a doublet?

(2) If there is more than a single doublet, is h in exactly the direction of v?

With regard to the first question, an example of a scenario where h does not originate purely from a doublet is that of doublet-singlet mixing, discussed in Section 3. Concerning the second question, we briefly discuss in this subsection the scenario of two Higgs doublet models (2HDMs).

In a 2HDM with Natural Flavor Conservation (NFC), there are three well-defined bases:

(1) The NFC basis (Φ_1, Φ_2), where each fermionic sector couples to either Φ_1 or Φ_2, but not to both.

(2) The Higgs basis (Φ_v, Φ_A), where $\langle\Phi_v\rangle = v/\sqrt{2}$ and $\langle\Phi_A\rangle = 0$.

(3) The mass basis (Φ_h, Φ_H), which is the mass basis for the *CP*-even neutral scalars h and H.

The rotation angle from the (Φ_1, Φ_2) to the (Φ_v, Φ_A) $[(\Phi_h, \Phi_H)]$ basis is denoted β [α]. We define κ_x via

$$\kappa_x \equiv \frac{g_{hxx}}{g_{hxx}^{SM}}\,. \tag{29}$$

In all 2HDMs we have ($V = W, Z$)

$$\begin{aligned} \kappa_V &= \sin(\beta-\alpha) \simeq 1 - \frac{1}{2}\cos^2(\beta-\alpha)\,, \\ \kappa_h &\simeq 1 - \frac{2m_A^2}{m_h^2}\cos^2(\beta-\alpha)\,. \end{aligned} \tag{30}$$

Note that for $m_A^2 \gg m_h^2$, we have $(m_A^2/m_h^2)\times\cos^2(\beta-\alpha) \simeq \cos(\beta-\alpha)$. In all NFC models, where by definition Φ_1 is the doublet that does not couple to the up sector,

$$\begin{aligned} \kappa_t &= \sin(\beta-\alpha) + \frac{\cos(\beta-\alpha)}{\tan\beta}\,, \\ \kappa_b &= \sin(\beta-\alpha) - \cos(\beta-\alpha)\tan\beta \quad \text{or} \quad \kappa_t\,, \\ \kappa_\tau &= \sin(\beta-\alpha) - \cos(\beta-\alpha)\tan\beta \quad \text{or} \quad \kappa_t\,, \end{aligned} \tag{31}$$

where the two options for the RHS of κ_b correspond to the cases where b couples to Φ_1 or Φ_2, respectively, and similarly for κ_τ. The largest deviations in these models arise in the down or charged lepton sector, if either or both couple to the doublet to which the up sector does not couple. If all fermions couple to Φ_2, then the largest deviation is expected in λ_h [48]. At the tree level, the results for the MSSM are the same as those of a type II 2HDM. We conclude that the most promising precision measurements of Higgs decays for obtaining hints of 2HDMs are those of $h \to b\bar{b}$ and $h \to \tau^+\tau^-$. Future projections of measuring y_b and y_τ in future experiments can be read from Table 7. An even more powerful probe of 2HDMs is the combination of these two couplings with a measurement of κ_V (see, Table 4). With $\kappa_Z = \sin(\beta-\alpha)$ measured very accurately, an accuracy of $\mathcal{O}(1\,\%)$ on y_τ will essentially constrain $\cos(\beta-\alpha)\tan\beta$ at that level in NFC models where the τ couples to Φ_1 only.

5.2 Is h elementary?

The question of Higgs compositeness is interesting in and of itself, but also in the context of mechanisms to explain the smallness of m_h^2 compared to m_{Pl}^2. Various models have been proposed where the Higgs is a pseudo-Goldstone boson which emerges from a strongly interacting sector [49–51]. An effective field theory framework for the strongly interacting light Higgs (SILH) incorporates the basic features of a large class of these models [52]. The low energy effective SILH Lagrangian depends on essentially two parameters: m_ρ, the mass scales of new resonances emerging from the strongly interacting sector, and g_ρ, their coupling. It is useful to define the dimensionless combination:

$$\xi = \frac{g_\rho^2 v^2}{m_\rho^2}\,. \tag{32}$$

The terms in the SILH Lagrangian that are relevant to our purposes are given by

$$\mathcal{L}_{\rm SILH} = \frac{c_{\rm H}\xi}{2v^2}\,\partial^\mu(\Phi^\dagger\Phi)\,\partial_\mu(\Phi^\dagger\Phi) + \frac{c_y\xi y_f}{v^2}\,\Phi^\dagger\Phi\overline{f_L}\Phi f_R + \text{h.c.} \tag{33}$$

Naive dimensional analysis (NDA) suggests that $c_{\rm H}$ and c_y are $\mathcal{O}(1)$. The theoretical framework only allows the parameters to be in the range

$$1 \leqslant g_\rho \leqslant 4\pi\,, \qquad \xi \leqslant 1\,. \tag{34}$$

Electroweak precision measurements give stronger constraints. The new physics contribution to $\hat{S}$ and $\hat{T}$ can be parameterized as follows [53]:

$$\begin{aligned}\Delta\hat{S} &= \frac{g^2}{96\pi^2}\,\xi\left[\log\left(\frac{\Lambda}{m_{\rm h}}\right) + 6\alpha\right] + \frac{m_W^2}{m_\rho^2}\,,\\ \Delta\hat{T} &= -\frac{g'^2}{32\pi^2}\,\xi\left[\log\left(\frac{\Lambda}{m_{\rm h}}\right) - 6\beta\,\frac{y_t^2}{g'^2}\right],\end{aligned} \tag{35}$$

where $\Lambda = 4\pi m_\rho/g_\rho$ and the coefficients α, $\beta = \mathcal{O}(1)$ and could have either sign. The resulting constraints read [53]

$$\xi \leqslant 0.15\,, \qquad m_\rho \geqslant 3\ \text{TeV} \tag{36}$$

when marginalizing over α and β (or $\xi \leqslant 0.025$ and $m_\rho \geqslant 4$ TeV for $\alpha = \beta = 0$). The modifications of the Higgs couplings are given by

$$\begin{aligned}\frac{\Delta g_V}{g_V^{\rm SM}} &= -\frac{c_H\xi}{2}\,, \qquad \frac{\Delta g_f}{g_f^{\rm SM}} = -\frac{c_H\xi}{2} - c_y\xi\,,\\ \frac{\Delta g_g}{g_g^{\rm SM}} &= -\frac{c_H\xi}{2} - c_y\xi\,, \qquad \frac{\Delta g_\gamma}{g_\gamma^{\rm SM}} = -\frac{c_H\xi}{2} + 0.3c_y\xi\,.\end{aligned} \tag{37}$$

Thus, the maximal possible deviations are [54]

$$\begin{aligned}\frac{\Delta g_V}{g_V^{\rm SM}} &\approx -0.08c_{\rm H}\,,\\ \frac{\Delta g_f}{g_f^{\rm SM}} = \frac{\Delta g_g}{g_g^{\rm SM}} &\approx -0.08 - 0.15\,\frac{c_y}{c_{\rm H}}\,,\\ \frac{\Delta g_\gamma}{g_\gamma^{\rm SM}} &\approx -0.08 + 0.05\,\frac{c_y}{c_{\rm H}}\,.\end{aligned} \tag{38}$$

For example, for $c_{\rm H} = c_y = 1$, the maximal deviations are -0.08, -0.20, and -0.03 for the g_V, $g_{f,g}$, and g_γ couplings, respectively. Estimates of the sensitivity to $c_H\xi$ of Higgs-related measurements for various colliders are collected in Table 9. Comparing this to the maximal possible deviations given above, it is clear that future colliders will probe this aspect in a very interesting regime. Currently, the precision obtained by ATLAS and CMS on κ_Z and κ_W is about 10% each [35, 36], resulting in a sensitivity of about 20% to $c_{\rm H}\xi$. Ref. [55] employs a more general framework, based on nonlinear shift symmetries acting on h and assuming custodial symmetry in the strong sector, and quotes the presently allowed 68% CL range as

$$\xi = -0.041^{+0.090}_{-0.094}\,. \tag{39}$$

Table 9. Summary of the sensitivity to ξ for various collider options, based on Ref. [53] but updated using recent projections of the κ_V sensitivity. See discussion in Section 5.2.

Collider	Energy	Luminosity, ab^{-1}	$\Delta g_V/g_V$, %	$(c_{\rm H}\xi)_{\rm max}$ [1σ]
HL-LHC	14 GeV	3	1.3	0.026
ILC	250 GeV	2	0.56	0.011
	+500 GeV	4	0.38	0.008
CLIC	380 GeV	1	0.6	0.012
	+1.4 TeV	2.5	0.6	0.012
	+3.0 TeV	5	0.6	0.012
FCC_{ee}	240 GeV	2×5.0	0.2	0.004
	+350 GeV	2.6	0.17	0.003
CEPC	240 GeV	2×5.6	0.25	0.005

Reference [53] compared the sensitivity of the Higgs-related measurements and the direct resonance searches at (and beyond) the LHC within the framework of composite Higgs models. They reach the conclusion that the Higgs-related measurements will be more sensitive for large g_ρ. Specifically, the indirect measurements explore novel territory for $g_\rho \gtrsim 4.5$.

5.3 What keeps $m_{\rm h}^2 \ll m_{\rm Pl}^2$?

If the SM is only a low energy effective theory, and at some high scale $\Lambda_{\rm NP}$ there are new degrees of freedom which couple to the Higgs boson, then the mass-squared of the Higgs boson gets corrections of $\mathcal{O}(\Lambda_{\rm NP}^2)$, and a fine-tuned cancellation with the bare μ^2 term is needed to keep the Higgs mass light. Possible solutions to this fine-tuning problem can be classified as symmetry-related mechanisms and dynamical scenarios. The two most intensively studied frameworks where the solution is symmetry related are composite Higgs and Supersymmetry. We discussed the composite Higgs framework in Section 5.2. As for Higgs couplings in the minimal supersymmetric SM (MSSM), the situation is similar to the 2HDM discussed in Section 5.1 with NFC type II, and with some additional constraints arising from relations to processes involving the supersymmetric partners of the SM degrees of freedom. Reference [54] obtained the maximal possible deviations of the h couplings, assuming that the scalar degrees of freedom of the second Higgs doublet are too heavy to be directly observed in the LHC. They obtain

$$\begin{aligned}1 - \kappa_V &\lesssim 0.01\,,\\ 1 - \kappa_t &\lesssim 0.03\,,\\ 1 - \kappa_b &\lesssim 0.1\text{–}1\,.\end{aligned} \tag{40}$$

A dynamical solution to the fine tuning problem is provided by relaxion models [56]. The Higgs mass depends on a time-dependent VEV of a scalar field which rolls until it stops at a value much smaller than the cut-off scale of the theory. Unlike models of composite Higgs or Supersymmetry, where many new degrees of freedom are predicted at a scale not much higher than the electroweak symmetry breaking scale, in this framework there is a single new scalar degree of freedom, constituting an SM-singlet, the relaxion $\phi_{\rm R}$. Much of the relevant phenomenology comes from the generic situation where the relaxion and the Higgs mix [19]. Thus, the relaxion inherits the Higgs couplings, suppressed by the small $\phi_{\rm R} - {\rm h}$ mixing angle. This scenario was discussed in Section 3, particularly in the case of $M_{\rm s} < M_{\rm h}/2$.

5.4 Was the electroweak phase transition (strongly) first order?

At a temperature of the order of 100 GeV, the Universe went through a transition from a high temperature symmetric phase ($\langle\Phi\rangle = 0$) to a state with broken electroweak symmetry ($\langle\Phi\rangle = v/\sqrt{2} \neq 0$). If the SM is a good low energy effective theory up to the TeV scale, then the electroweak phase transition (EWPT) is a crossover transition. If, on the other hand, the EWPT was first-order, then electroweak baryogenesis was possible. In fact, successful EWBG requires that the phase transition be strongly first order,

$$\frac{v(T_c)}{T_c} \gtrsim 1\,, \tag{41}$$

where T_c is the temperature at which the phase transition takes place. This requirement usually implies new degrees of freedom that are not much heavier than the EW scale and which couple to the Higgs field with a coupling that is not small. The new physics that can make a first-order EWPT can be broadly classified into four classes [57], distinguished by the physics that is responsible for generating the barrier between the EW-symmetric and EW-breaking minima:

• Thermally driven. New bosonic degrees of freedom generate a finite-temperature term in the effective potential of the form $-T(h^2)^{3/2}$.

• Tree-level renormalizable operators. Additional scalars, typically $SU(2)_L$-singlets or doublets, mix with the Higgs boson and generate an effective, temperature-independent, h^3 term.

• Tree level nonrenormalizable operators. The most intensively studied example is a dimension-six term $(\Phi^\dagger\Phi)^3$ (with a negative λ for the $\lambda(\Phi^\dagger\Phi)^2$).

• Loop corrections. The most intensively studied example is an effective term of the form $\kappa h^4 \ln(h^2/M^2)$ in the Higgs potential.

Loops involving scalar particles induce a cubic term in the effective potential at high temperature that can modify the EWPT into a first-order one (see, for example, Ref. [29]). Consider then a new scalar S, with coupling to the Higgs field Φ:

$$V_{S\Phi} = \kappa|S|^2|\Phi|^2\,. \tag{42}$$

To make the phase transition first-order, we need $\kappa = \mathcal{O}(1)$ and $m_S \lesssim 400$ GeV. This term modifies the following Higgs observables:

1. If S is colored, the hgg coupling is modified. Thus, at hadron colliders, a measurement of μ_{ggF} is best suited to probe this scenario, which is expected to have a precision of about 2% at HL-LHC. At lepton colliders, the best observable is $BR(h \to gg)$, which can be probed with a precision of about 1.5–2.5%.

2. If S is electromagnetically charged, the $h\gamma\gamma$ coupling is modified. Thus, a measurement of $BR(h \to \gamma\gamma)$ is best suited to probe this scenario. At HL-LHC, a precision of about 2.6% is expected, and lepton colliders are not expected to improve this significantly. A substantial improvement is expected from FCC_{hh} with about 0.5%.

3. Independently of the quantum numbers of S, the hZZ coupling will be modified, since S renormalizes the Higgs wavefunction [10, 58]. The case where S is neither colored nor electromagnetically charged was discussed in Section 3.

Most models of strongly first-order EWPT due to renormalizable tree-level operators have by now been ruled out by measurements of the invisible Higgs decays or by the bounds on the mixing with singlet scalars, discussed in Section 3. For models of strongly first-order EWPT due to non-renormalizable tree-level operators,

$$V = \mu^2(\Phi^\dagger\Phi) + \lambda(\Phi^\dagger\Phi)^2 + \frac{\rho}{\Lambda^2}(\Phi^\dagger\Phi)^3\,, \tag{43}$$

the main consequence is a modification of the relation between the Higgs mass, the VEV, and the trilinear Higgs self-coupling:

$$\lambda_{hhh} = 3\,\frac{m_h^2}{v} + 6\rho\,\frac{v^3}{\Lambda^2}\,. \tag{44}$$

The required size of $\rho v^2/\Lambda^2$ is such that a deviation of $\mathcal{O}(1)$ in λ_{hhh} are predicted. Table 10 summarizes the expected sensitivity of various future colliders.

Table 10. Summary of the sensitivity to λ_{hhh} for various collider options.*

Collider	$\sqrt{s}$	$\Delta\lambda_{hhh}/\lambda_{hhh}$, %
HL-LHC	14 TeV	±50
ILC	500 GeV	±17
CLIC	3.0 TeV	$^{+11}_{-7}$
FCC_{ee}	240 + 365 GeV	±40
HE-LHC	27 TeV	±(10–20)
FCC_{hh}	100 TeV	±5

* Given are the collider, the center-of-mass energy, the integrated luminosity, and the precision that is expected to be achieved on λ_{hhh}. For all colliders, except FCC_{ee}, the result is based on di-Higgs measurements. For FCC_{ee}, it is based on the $\sqrt{s}$ dependence of higher order corrections to the Zh cross section. In all cases, the luminosity quoted is that of the sum of the experiments. The values correspond to the luminosities given in Section 2.

5.5 Do *CP* violating h interactions generate the baryon asymmetry?

Complex Yukawa couplings could play a *CP*-violating role in electroweak baryogenesis (see, e.g., Refs [61–64]). Various suggestions of how to measure such *CP*-violating Higgs interactions have been made, in particular for $h\tau\tau$ and htt couplings (see, e.g., Refs [65–74]).

The ATLAS collaboration [75] has recently estimated the accuracy of measuring the *CP*-violating mixing angle

$$\mathcal{L}_{h\tau\tau} = g_{h\tau\tau}\left[\cos(\phi_\tau)\,\bar\tau\tau + \sin(\phi_\tau)\,\bar\tau i\gamma_5\tau\right] h\,. \tag{45}$$

With 3 ab^{-1} at $\sqrt{s} = 14$ TeV, ϕ_τ can be measured with a statistical precision between ±18° and ±33°, depending on the energy resolution of the π^0 achieved in the reconstruction at high pile-up.

6. Conclusions

A list of interesting theoretical questions, and a partial list of observables that are most relevant to making progress on these questions, are summarized in Table 11.

Our review of what can be learned from Higgs precision measurements led us to three important conclusions, independent of the particular experiments that will perform these measurements:

• The Higgs program, which is guaranteed program of any future collider, touches some of the most significant open questions in particle physics and cosmology. In particular,

Table 11. A list of interesting theoretical questions and a partial list of observables that are most relevant to making progress on these questions. κ_3 (κ_ℓ) stands for third (first or second) generation couplings. μ_{4f} stands for the processes $h \to SS \to \bar{f}_1 f_1 \bar{f}_2 f_2$. For more details, see the text.

Question	κ_V	κ_3	κ_g	κ_γ	λ_{hhh}	σ_{hZ}	BR_{inv}	BR_{und}	κ_ℓ	μ_{4f}	$BR_{\tau\mu}$	Γ_h
Is h Alone?	+	+			+	+				+		+
Is h elementary?	+	+	+	+		+						
Why $m_h^2 \ll m_{Pl}^2$?	+	+					+	+		+		+
1st order EWPT?			+	+	+	+				+		
CPV?		+(*CP*)										
Light singlets?							+	+	+	+		+
Flavor puzzles?		+							+		+	

this program may lead to progress on two puzzles of particle cosmology: dark matter and the baryon asymmetry.

• No Higgs-related measurement will go unnoticed. Each of the production modes and each of the decay modes carries in it information that is relevant to important questions. Higgs decays into two bosons, two fermions, invisible modes, four fermions, as well as Higgs production by gluon-gluon fusion, $t\bar{t}h$, and di-Higgs production, all of these (and other measurements) are highly valuable for better understanding particle physics and cosmology.

• For many of the interesting observables, the proposed future colliders significantly extend the sensitivity beyond that reachable by the HL-LHC alone.

Acknowledgments

We thank the members of the Scientific Policy Committee (SPC) of CERN for initiating discussions that led to this work, and for comments on the manuscript. We thank the participants in the workshop "Voyages Beyond the Standard Model II," and Gilad Perez and Georg Weiglein for useful discussions and comments on the manuscript. BH acknowledges the support from the Deutsche Forschungsgemeinschaft (DFG, German Research Foundation) under Germany's Excellence Strategy — EXC 2121 "Quantum Universe" — 390833306. YN is the Amos de-Shalit Chair of theoretical physics, and is supported by grants from the Israel Science Foundation (grant number 394/16), the United States-Israel Binational Science Foundation (BSF), Jerusalem, Israel (grant number 2014230), and the I-CORE program of the Planning and Budgeting Committee and the Israel Science Foundation (grant number 1937/12).

References

1. Aad G et al. (ATLAS Collab.) *Phys. Lett. B* **716** 1 (2012); arXiv:1207.7214
2. Chatrchyan S et al. (CMS Collab.) *Phys. Lett. B* **716** 30 (2012); arXiv:1207.7235
3. Englert F, Brout R *Phys. Rev. Lett.* **13** 321 (1964)
4. Higgs P W *Phys. Rev. Lett.* **13** 508 (1964)
5. Bordry F et al., arXiv:1810.13022
6. Bambade P et al., arXiv:1903.01629
7. CEPC Study Group, arXiv:1811.10545
8. Mangano M et al., CERN-ACC-2018-0056
9. Huang P, Long A J, Wang L-T *Phys. Rev. D* **94** 075008 (2016); arXiv:1608.06619
10. Craig N, Englert C, McCullough M *Phys. Rev. Lett.* **111** 121803 (2013); arXiv:1305.5251
11. Curtin D, Meade P, Yu C-T *J. High Energ. Phys.* **2014** (11) 127 (2014); arXiv:1409.0005
12. Fan J, Reece M, Wang L-T *J. High Energ. Phys.* **2015** (08) 152 (2015); arXiv:1412.3107
13. Frugiuele C et al. *J. High Energ. Phys.* **2018** (10) 151 (2018); arXiv:1807.10842
14. Sirunyan A M et al. (CMS Collab.) *Phys. Lett. B* **793** 520 (2019); arXiv:1809.05937
15. Aaboud M et al. (ATLAS) *Phys. Lett. B* **793** 499 (2019); arXiv:1809.06682
16. Robson A, Roloff P, arXiv:1812.01644
17. Barklow T et al. *Phys. Rev. D* **97** 053003 (2018); arXiv:1708.08912
18. Bechtle P et al. *J. High Energ. Phys.* **2014** (11) 39 (2014); arXiv:1403.1582
19. Flacke T et al. *J. High Energ. Phys.* **2017** (06) 50 (2017); arXiv:1610.02025
20. ATLAS, CMS Collab., arXiv:1902.10229
21. Sirunyan A M et al. (CMS Collab.) *Phys. Lett. B* **785** 462 (2018); arXiv:1805.10191
22. Khachatryan V (CMS Collab.) *J. High Energ. Phys.* **2017** (10) 76 (2017); arXiv:1701.02032
23. Aaboud M et al. (ATLAS Collab.) *Phys. Lett. B* **790** 1 (2019); arXiv:1807.00539
24. Sirunyan A M et al. (CMS Collab.) *J. High Energ. Phys.* **2018** (11) 18 (2018); arXiv:1805.04865
25. Aaboud M et al (ATLAS Collab.) *Phys. Lett. B* **782** 750 (2018); arXiv:1803.11145
26. Sirunyan et al. (CMS Collab.) *Phys. Rev. D* **99** 112003 (2019); arXiv:1901.00174
27. Cepeda M et al. (Physics of the HL-LHC Working Group), arXiv:1902.00134
28. Aad G et al. (ATLAS Colab., CMS Collab.) *J. High Energ. Phys.* **2016** (08) 45 (2016); arXiv:1606.02266
29. Katz A, Perelstein M *J. High Energ. Phys.* **2014** (07) 108 (2014); arXiv:1401.1827
30. Nir Y *Phys. Scripta* **2013** (T158) 014005 (2013)
31. Dery A et al. *J. High Energ. Phys.* **2013** (05) 39 (2013); arXiv:1302.3229
32. Agashe K et al. (Top Quark Working Group), arXiv:1311.2028
33. Dery A et al. *J. High Energ. Phys.* **2013** (08) 6 (2013); arXiv:1304.6727
34. Dery A et al. *Phys. Rev. D* **90** 115022 (2014); arXiv:1408.1371
35. Sirunyan A M et al. (CMS Collab.) *Eur. Phys. J. C* **79** 421 (2019); arXiv:1809.10733
36. ATLAS Collab., ATLAS Note ATLAS-CONF-2018-031
37. Charles T K et al. (CLIC Collab., CLICdp Collab.) *The Compact Linear Collider* (*CLIC*) *— 2018 Summary Report* (CERN Yellow Reports: Monographs, Vol. 2/2018, CERN-2018-005-M, Eds P N Burrows et al.) (Geneva: CERN, 2018) https//doi.org/10.23731/CYRM-2018-002; arXiv:1812.06018
38. Duarte-Campderros J et al., arXiv:1811.09636
39. Klein U "FCC-eh as a Higgs facility", in *FCC Week, The Fourth Annual Meeting of the Future Circular Collider Study, 9–13 April 2018, Amsterdam*
40. Aaboud M et al. (ATLAS Collab.) *Phys. Rev. Lett.* **120** 211802 (2018); arXiv:1802.04329
41. Perez G et al. *Phys. Rev. D* **92** 033016 (2015); arXiv:1503.00290
42. Khachatryan V et al. (CMS Collab.) *Phys. Lett. B* **744** 184 (2015); arXiv:1410.6679
43. Aaboud M et al. (ATLAS Collab.) *J. High Energ. Phys.* **2019** 123 (2019); arXiv:1812.11568
44. Azzi P et al. (HL-LHC Collab., HE-LHC Working Group), arXiv:1902.04070
45. Aad G et al. (ATLAS Collab.) *Eur. Phys. J. C* **77** 70 (2017); arXiv:1604.07730
46. Sirunyan A M et al. (CMS Collab.) *J. High Energ. Phys.* **2018** (06) 1 (2018); arXiv:1712.07173

47. Khachatryan V et al. (CMS Collab.) *Phys. Lett. B* **763** 472 (2016); arXiv:1607.03561
48. Efrati A, Nir Y, arXiv:1401.0935
49. Arkani-Hamed N et al. *J. High Energ. Phys.* (07) 034 (2002)
50. Contino R, Nomura Y, Pomarol A *Nucl. Phys. B* **671** 148 (2003)
51. Agashe K, Contino R, Pomarol A *Nucl. Phys. B* **719** 165 (2005)
52. Giudice G F et al. *J. High Energ. Phys.* (06) 045 (2007)
53. Thamm A, Torre R, Wulzer A *J. High Energ. Phys.* **2015** (07) 100 (2015); arXiv:1502.01701
54. Gupta R S, Rzehak H, Wells J D *Phys. Rev. D* **86** 095001 (2012); arXiv:1206.3560
55. Liu D, Low I, Yin Z *J. High Energ. Phys.* **2019** (05) 170 (2019); arXiv:1809.09126
56. Graham P W, Kaplan D E, Rajendran S *Phys. Rev. Lett.* **115** 221801 (2015); arXiv:1504.07551
57. Chung D J H, Long A J, Wang L-T *Phys. Rev. D* **87** 023509 (2013); arXiv:1209.1819
58. Englert C, McCullough M *J. High Energ. Phys.* **2013** (07) 168 (2013); arXiv:1303.1526
59. Profumo S et al. *Phys. Rev. D* **91** 035018 (2015); arXiv:1407.5342
60. Kotwal A V et al. *Phys. Rev. D* **94** 035022 (2016); arXiv:1605.06123
61. Shu J, Zhang Y *Phys. Rev. Lett.* **111** 091801 (2013); arXiv:1304.0773
62. Kobakhidze A, Wu L, Yue J *J. High Energ. Phys.* **2016** (04) 11 (2016); arXiv:1512.08922
63. Chiang C-W, Fuyuto K, Senaha E *Phys. Lett. B* **762** 315 (2016); arXiv:1607.07316
64. Guo H-K et al. *Phys. Rev. D* **96** 115034 (2017); arXiv:1609.09849
65. Harnik R et al. *Phys. Rev. D* **88** 076009 (2013); arXiv:1308.1094
66. Demartin F et al. *Eur. Phys. J. C* **74** 3065 (2014)Ì arXiv:1407.5089
67. Buckley M R, Gonçalves D *Phys. Rev. Lett.* **116** 091801 (2016); arXiv:1507.07926
68. Amor Dos Santos S et al. *Phys. Rev. D* **96** 013004 (2017); arXiv:1704.03565
69. Huang F P et al. *Phys. Rev. D* **93** 103515 (2016); arXiv:1511.03969
70. Hayreter A, He X-G, Valencia G *Phys. Lett. B* **760** 175 (2016); arXiv:1603.06326
71. Hayreter A, He X-G, Valencia G *Phys. Rev. D* **94** 075002 (2016); arXiv:1606.00951
72. Gonçalves D, Kim J H, Kong K *J. High Energ. Phys.* **2018** (06) 79 (2018); arXiv:1804.05874
73. Bernlochner F U et al. *Phys. Lett. B* **790** 372 (2019); arXiv:1808.06577
74. de Blas J et al. *The CLIC Potential for New Physics* (CERN Yellow Reports: Monographs, Vol. 3/2018, CERN-2018-009-M, Eds J de Blas et al.) (Geneva: CERN, 2018) http://dx.doi.org/10.23731/CYRM-2018-003; arXiv:1812.02093
75. The ATLAS Collab., ATLAS-PHYS-PUB-2019-008